Chapter I.
Examples and Numerical Experiments

This chapter introduces some interesting examples of differential equations and illustrates different types of qualitative behaviour of numerical methods. We deliberately consider only very simple numerical methods of orders 1 and 2 to emphasize the qualitative aspects of the experiments. The same effects (on a different scale) occur with more sophisticated higher-order integration schemes. The experiments presented here should serve as a motivation for the theoretical and practical investigations of later chapters. The reader is encouraged to repeat the experiments or to invent similar ones.

I.1 First Problems and Methods

> Numerical applications of the case of two dependent variables are not easily obtained. (A.J. Lotka 1925, p. 79)

Our first problems, the Lotka–Volterra model and the pendulum equation, are differential equations in two dimensions and show already many interesting geometric properties. Our first methods are various variants of the Euler method, the midpoint rule, and the Störmer–Verlet scheme.

I.1.1 The Lotka–Volterra Model

We start with an equation from mathematical biology which models the growth of animal species. If a real variable $u(t)$ is to represent the number of individuals of a certain species at time t, the simplest assumption about its evolution is $du/dt = u \cdot \alpha$, where α is the reproduction rate. A constant α leads to exponential growth. In the case of more species living together, the reproduction rates will also depend on the population numbers of the *other* species. For example, for two species with $u(t)$ denoting the number of predators and $v(t)$ the number of prey, a plausible assumption is made by the *Lotka–Volterra model*

$$\begin{aligned} \dot{u} &= u(v-2) \\ \dot{v} &= v(1-u), \end{aligned} \tag{1.1}$$

where the dots on u and v stand for differentiation with respect to time. (We have chosen the constants 2 and 1 in (1.1) arbitrarily.) A.J. Lotka (1925, Chap. VIII) used

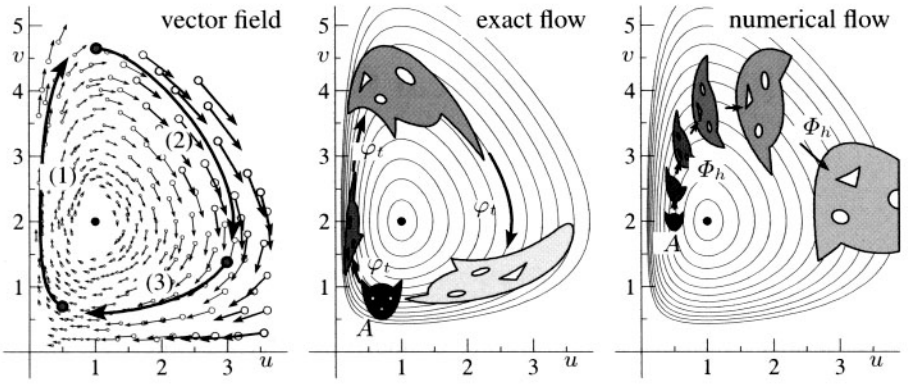

Fig. 1.1. Vector field, exact flow, and numerical flow for the Lotka–Volterra model (1.1)

this model to study parasitic invasion of insect species, and, with its help, V. Volterra (1927) explained curious fishing data from the upper Adriatic Sea following World War I.

Equations (1.1) constitute an autonomous system of differential equations. In general, we write such a system in the form

$$\dot{y} = f(y) \,. \tag{1.2}$$

Every y represents a point in the *phase space*, in equation (1.1) above $y = (u, v)$ is in the phase plane $\mathbb{R}^2$. The vector-valued function $f(y)$ represents a *vector field* which, at any point of the phase space, prescribes the velocity (direction and speed) of the solution $y(t)$ that passes through that point (see the first picture of Fig. 1.1).

For the Lotka–Volterra model, we observe that the system cycles through three stages: (1) the prey population increases; (2) the predator population increases by feeding on the prey; (3) the predator population diminishes due to lack of food.

Flow of the System. A fundamental concept is the *flow* over time t. This is the mapping which, to any point y_0 in the phase space, associates the value $y(t)$ of the solution with initial value $y(0) = y_0$. This map, denoted by φ_t, is thus defined by

$$\varphi_t(y_0) = y(t) \quad \text{if} \quad y(0) = y_0. \tag{1.3}$$

The second picture of Fig. 1.1 shows the results of three iterations of φ_t (with $t = 1.3$) for the Lotka–Volterra problem, for a set of initial values $y_0 = (u_0, v_0)$ forming an animal-shaped set A.[1]

Invariants. If we divide the two equations of (1.1) by each other, we obtain a single equation between the variables u and v. After separation of variables we get

$$0 = \frac{1-u}{u}\,\dot{u} - \frac{v-2}{v}\,\dot{v} = \frac{d}{dt}\,I(u,v)$$

[1] This cat came to fame through Arnold (1963).

where

$$I(u,v) = \ln u - u + 2\ln v - v, \tag{1.4}$$

so that $I(u(t),v(t)) = Const$ for all t. We call the function I an *invariant* of the system (1.1). Every solution of (1.1) thus lies on a level curve of (1.4). Some of these curves are drawn in the pictures of Fig. 1.1. Since the level curves are closed, all solutions of (1.1) are periodic.

I.1.2 First Numerical Methods

Explicit Euler Method. The simplest of all numerical methods for the system (1.2) is the method formulated by Euler (1768),

$$y_{n+1} = y_n + hf(y_n). \tag{1.5}$$

It uses a constant step size h to compute, one after the other, approximations y_1, y_2, y_3, ... to the values $y(h)$, $y(2h)$, $y(3h)$, ... of the solution starting from a given initial value $y(0) = y_0$. The method is called the *explicit Euler method*, because the approximation y_{n+1} is computed using an explicit evaluation of f at the already known value y_n. Such a formula represents a mapping

$$\Phi_h : y_n \mapsto y_{n+1},$$

which we call the *discrete* or *numerical flow*. Some iterations of the discrete flow for the Lotka–Volterra problem (1.1) (with $h = 0.5$) are represented in the third picture of Fig. 1.1.

Implicit Euler Method. The *implicit Euler method*

$$y_{n+1} = y_n + hf(y_{n+1}), \tag{1.6}$$

is known for its all-damping stability properties. In contrast to (1.5), the approximation y_{n+1} is defined implicitly by (1.6), and the implementation requires the numerical solution of a nonlinear system of equations.

Implicit Midpoint Rule. Taking the mean of y_n and y_{n+1} in the argument of f, we get the *implicit midpoint rule*

$$y_{n+1} = y_n + hf\Big(\frac{y_n + y_{n+1}}{2}\Big). \tag{1.7}$$

It is a *symmetric* method, which means that the formula is left unaltered after exchanging $y_n \leftrightarrow y_{n+1}$ and $h \leftrightarrow -h$ (more on symmetric methods in Chap. V).

Symplectic Euler Methods. For *partitioned* systems

$$\begin{aligned} \dot u &= a(u,v) \\ \dot v &= b(u,v), \end{aligned} \tag{1.8}$$

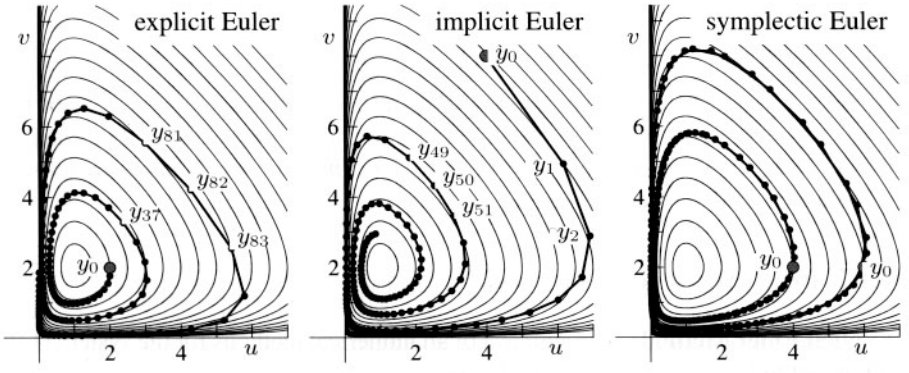

Fig. 1.2. Solutions of the Lotka–Volterra equations (1.1) (step sizes $h = 0.12$; initial values $(2, 2)$ for the explicit Euler method, $(4, 8)$ for the implicit Euler method, $(4, 2)$ and $(6, 2)$ for the symplectic Euler method)

such as the problem (1.1), we consider also *partitioned* Euler methods

$$\begin{aligned} u_{n+1} &= u_n + ha(u_n, v_{n+1}) \\ v_{n+1} &= v_n + hb(u_n, v_{n+1}), \end{aligned} \qquad \text{or} \qquad \begin{aligned} u_{n+1} &= u_n + ha(u_{n+1}, v_n) \\ v_{n+1} &= v_n + hb(u_{n+1}, v_n), \end{aligned} \tag{1.9}$$

which treat one variable by the implicit and the other variable by the explicit Euler method. In view of an important property of this method, discovered by de Vogelaere (1956) and to be discussed in Chap. VI, we call them *symplectic Euler methods*.

Numerical Example for the Lotka–Volterra Problem. Our first numerical experiment shows the behaviour of the various numerical methods applied to the Lotka–Volterra problem. In particular, we are interested in the preservation of the invariant I over long times. Fig. 1.2 plots the numerical approximations of the first 125 steps with the above numerical methods applied to (1.1), all with constant step sizes. We observe that the explicit and implicit Euler methods show wrong qualitative behaviour. The numerical solution either spirals outwards or inwards. The symplectic Euler method (implicit in u and explicit in v), however, gives a numerical solution that lies apparently on a closed curve as does the exact solution. Note that the curves of the numerical and exact solutions do not coincide.

I.1.3 The Pendulum as a Hamiltonian System

A great deal of attention in this book will be addressed to Hamiltonian problems, and our next examples will be of this type. These problems are of the form

$$\dot{p} = -H_q(p, q), \qquad \dot{q} = H_p(p, q), \tag{1.10}$$

where the *Hamiltonian* $H(p_1, \ldots, p_d, q_1, \ldots q_d)$ represents the total energy; q_i are the position coordinates and p_i the momenta for $i = 1, \ldots, d$, with d the number of

degrees of freedom; H_p and H_q are the vectors of partial derivatives. One verifies easily by differentiation (see Sect. IV.1) that, along the solution curves of (1.10),

$$H\big(p(t), q(t)\big) = Const, \tag{1.11}$$

i.e., the Hamiltonian is an invariant or a *first integral*. More details about Hamiltonian systems and their derivation from Lagrangian mechanics will be given in Sect. VI.1.

Pendulum. The mathematical pendulum (mass $m = 1$, massless rod of length $\ell = 1$, gravitational acceleration $g = 1$) is a system with one degree of freedom having the Hamiltonian

$$H(p, q) = \frac{1}{2}p^2 - \cos q, \tag{1.12}$$

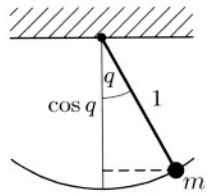

so that the equations of motion (1.10) become

$$\dot{p} = -\sin q, \qquad \dot{q} = p. \tag{1.13}$$

Since the vector field (1.13) is 2π-periodic in q, it is natural to consider q as a variable on the circle S^1. Hence, the phase space of points (p, q) becomes the cylinder $\mathbb{R} \times S^1$. Fig. 1.3 shows some level curves of $H(p, q)$. By (1.11), the solution curves of the problem (1.13) lie on such level curves.

exact flow | explicit Euler | symplectic Euler

Fig. 1.3. Exact and numerical flow for the pendulum problem (1.13); step sizes $h = t = 1$

Area Preservation. Figure 1.3 (first picture) illustrates that the exact flow of a Hamiltonian system (1.10) is area preserving. This can be explained as follows: the derivative of the flow φ_t with respect to initial values (p, q),

$$\varphi_t'(p, q) = \frac{\partial\big(p(t), q(t)\big)}{\partial(p, q)},$$

satisfies the variational equation [2]

$$\dot{\varphi}'_t(p,q) = \begin{pmatrix} -H_{pq} & -H_{qq} \\ H_{pp} & H_{qp} \end{pmatrix} \varphi'_t(p,q)\,,$$

where the second partial derivatives of H are evaluated at $\varphi_t(p,q)$. In the case of one degree of freedom ($d = 1$), a simple computation shows that

$$\frac{d}{dt} \det \varphi'_t(p,q) = \frac{d}{dt}\Big(\frac{\partial p(t)}{\partial p}\,\frac{\partial q(t)}{\partial q} - \frac{\partial p(t)}{\partial q}\,\frac{\partial q(t)}{\partial p} \Big) = \ldots = 0.$$

Since φ_0 is the identity, this implies $\det \varphi'_t(p,q) = 1$ for all t, which means that the flow $\varphi_t(p,q)$ is an *area-preserving* mapping.

The last two pictures of Fig. 1.3 show numerical flows. The explicit Euler method is clearly seen not to preserve area but the symplectic Euler method is (this will be proved in Sect. VI.3). One of the aims of 'geometric integration' is the study of numerical integrators that preserve such types of qualitative behaviour of the exact flow.

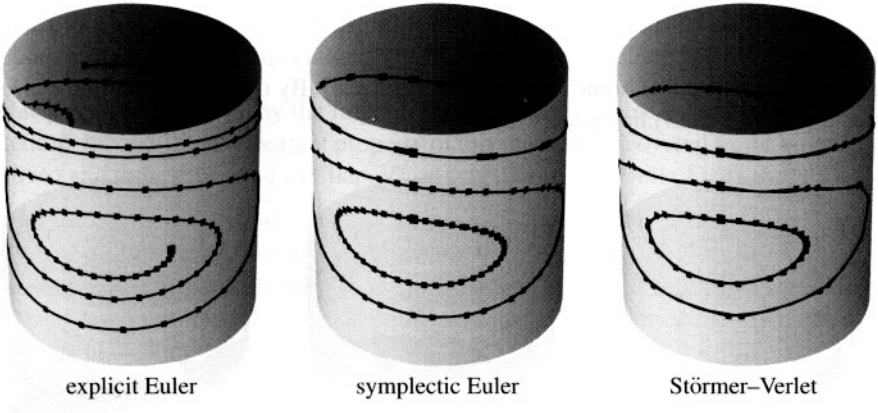

Fig. 1.4. Solutions of the pendulum problem (1.13); explicit Euler with step size $h = 0.2$, initial value $(p_0, q_0) = (0, 0.5)$; symplectic Euler with $h = 0.3$ and initial values $q_0 = 0$, $p_0 = 0.7, 1.4, 2.1$; Störmer–Verlet with $h = 0.6$

Numerical Experiment. We apply the above numerical methods to the pendulum equations (see Fig. 1.4). Similar to the computations for the Lotka–Volterra equations, we observe that the numerical solutions of the explicit Euler and of the implicit Euler method (not drawn in Fig. 1.4) spiral either outwards or inwards. The symplectic Euler method shows the correct qualitative behaviour, but destroys the left-right symmetry of the problem. The Störmer–Verlet scheme, which we discuss next, works perfectly even with doubled step size.

[2] As is common in the study of mechanical problems, we use *dots* for denoting time-derivatives, and we use *primes* for denoting derivatives with respect to other variables.

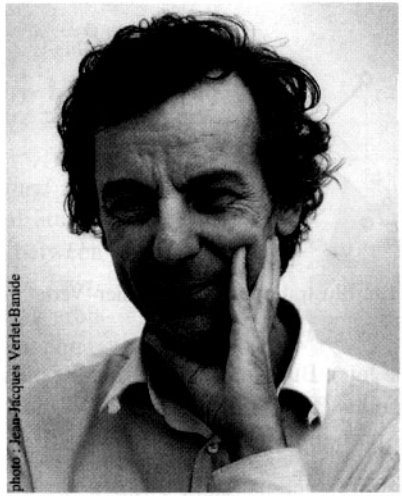

Fig. 1.5. Carl Störmer (left picture), born: 3 September 1874 in Skien (Norway), died: 13 August 1957.
Loup Verlet (right picture), born: 24 May 1931 in Paris

I.1.4 The Störmer–Verlet Scheme

The above equations (1.13) for the pendulum are of the form

$$\begin{aligned} \dot{p} &= f(q) \\ \dot{q} &= p \end{aligned} \qquad \text{or} \qquad \ddot{q} = f(q) \tag{1.14}$$

which is the important special case of a second order differential equation. The most natural discretization of (1.14) is

$$q_{n+1} - 2q_n + q_{n-1} = h^2 f(q_n), \tag{1.15}$$

which is just obtained by replacing the second derivative in (1.14) by the central second-order difference quotient. This basic method, or its equivalent formulation given below, is called the *Störmer method* in astronomy, the *Verlet method*[3] in molecular dynamics, the *leap-frog method* in the context of partial differential equations, and it has further names in other areas (see Hairer, Lubich & Wanner (2003), p. 402). C. Störmer (1907) used higher-order variants for numerical computations concerning the aurora borealis. L. Verlet (1967) proposed this method for computations in molecular dynamics, where it has become by far the most widely used integration scheme.

Geometrically, the Störmer–Verlet method can be seen as produced by parabolas, which in the points t_n possess the right second derivative $f(q_n)$ (see Fig. 1.6

[3] Irony of fate: Professor Loup Verlet, who later became interested in the history of science, discovered precisely "his" method in Newton's *Principia* (Book I, figure for Theorem I, see Sect. I.2.1 below).

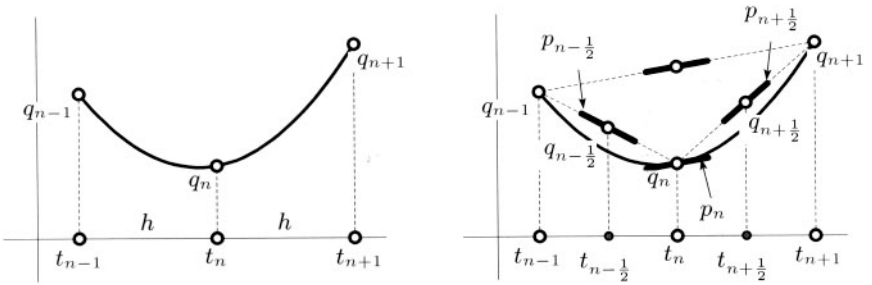

Fig. 1.6. Illustration for the Störmer–Verlet method

to the left). But we can also think of polygons, which possess the right slope in the midpoints (Fig. 1.6 to the right).

Approximations to the derivative $p = \dot{q}$ are simply obtained by

$$p_n = \frac{q_{n+1} - q_{n-1}}{2h} \qquad \text{and} \qquad p_{n+1/2} = \frac{q_{n+1} - q_n}{h}. \tag{1.16}$$

One-Step Formulation. The Störmer–Verlet method admits a one-step formulation which is useful for actual computations. The value q_n together with the slope p_n and the second derivative $f(q_n)$, all at t_n, uniquely determine the parabola and hence also the approximation (p_{n+1}, q_{n+1}) at t_{n+1}. Writing (1.15) as $p_{n+1/2} - p_{n-1/2} = hf(q_n)$ and using $p_{n+1/2} + p_{n-1/2} = 2p_n$, we get by elimination of either $p_{n+1/2}$ or $p_{n-1/2}$ the formulae

$$\begin{aligned} p_{n+1/2} &= p_n + \frac{h}{2} f(q_n) \\ q_{n+1} &= q_n + h p_{n+1/2} \\ p_{n+1} &= p_{n+1/2} + \frac{h}{2} f(q_{n+1}) \end{aligned} \tag{1.17}$$

which is an explicit one-step method $\Phi_h : (q_n, p_n) \mapsto (q_{n+1}, p_{n+1})$ for the corresponding first order system of (1.14). If one is not interested in the values p_n of the derivative, the first and third equations in (1.17) can be replaced by

$$p_{n+1/2} = p_{n-1/2} + h\, f(q_n).$$

I.2 The Kepler Problem and the Outer Solar System

> I awoke as if from sleep, a new light broke on me. (J. Kepler; quoted from J.L.E. Dreyer, *A history of astronomy*, 1906, Dover 1953, p. 391)

One of the great achievements in the history of science was the discovery of the laws of J. Kepler (1609), based on many precise measurements of the positions of Mars by Tycho Brahe and himself. The planets move in *elliptic orbits* with the sun at one of the foci (Kepler's first law)

$$r = \frac{d}{1 + e\cos\varphi} = a - ae\cos E, \tag{2.1}$$

(where a = great axis, e = eccentricity, $b = a\sqrt{1-e^2}$, $d = b\sqrt{1-e^2} = a(1-e^2)$, E = eccentric anomaly, φ = true anomaly).

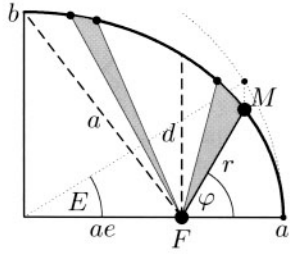

Newton (*Principia* 1687) then *explained* this motion by his general law of gravitational attraction (proportional to $1/r^2$) and the relation between forces and acceleration (the "Lex II" of the *Principia*). This then opened the way for treating arbitrary celestial motions by solving differential equations.

Two-Body Problem. For computing the motion of two bodies which attract each other, we choose one of the bodies as the centre of our coordinate system; the motion will then stay in a plane (Exercise 3) and we can use two-dimensional coordinates $q = (q_1, q_2)$ for the position of the second body. Newton's laws, with a suitable normalization, then yield the following differential equations

$$\ddot{q}_1 = -\frac{q_1}{(q_1^2+q_2^2)^{3/2}}, \qquad \ddot{q}_2 = -\frac{q_2}{(q_1^2+q_2^2)^{3/2}}. \tag{2.2}$$

This is equivalent to a Hamiltonian system with the Hamiltonian

$$H(p_1,p_2,q_1,q_2) = \frac{1}{2}\left(p_1^2+p_2^2\right) - \frac{1}{\sqrt{q_1^2+q_2^2}}, \qquad p_i = \dot{q}_i. \tag{2.3}$$

I.2.1 Angular Momentum and Kepler's Second Law

The system has not only the total energy $H(p,q)$ as a first integral, but also the angular momentum

$$L(p_1,p_2,q_1,q_2) = q_1p_2 - q_2p_1. \tag{2.4}$$

This can be checked by differentiation and is nothing other than *Kepler's second law*, which says that the ray FM sweeps equal areas in equal times (see the little picture at the beginning of Sect. I.2).

A beautiful *geometric* justification of this law is due to I. Newton[4] (*Principia* (1687), Book I, figure for Theorem I). The idea is to apply the Störmer–Verlet scheme (1.15) to the equations (2.2) (see Fig. 2.1). By hypothesis, the diagonal of the parallelogram $q_{n-1}q_nq_{n+1}$, which is $(q_{n+1}-q_n)-(q_n-q_{n-1}) = q_{n+1}-2q_n+q_{n-1} = Const\cdot f(q_n)$, points towards the sun S. Therefore, the altitudes of the triangles $q_{n-1}q_nS$ and $q_{n+1}q_nS$ are equal. Since they have the common base q_nS, they also have equal areas. Hence

$$\det(q_{n-1}, q_n - q_{n-1}) = \det(q_n, q_{n+1} - q_n)$$

and by passing to the limit $h \to 0$ we see that $\det(q,p) = Const$. This is (2.4).

[4] We are grateful to a private communication of L. Verlet for this reference

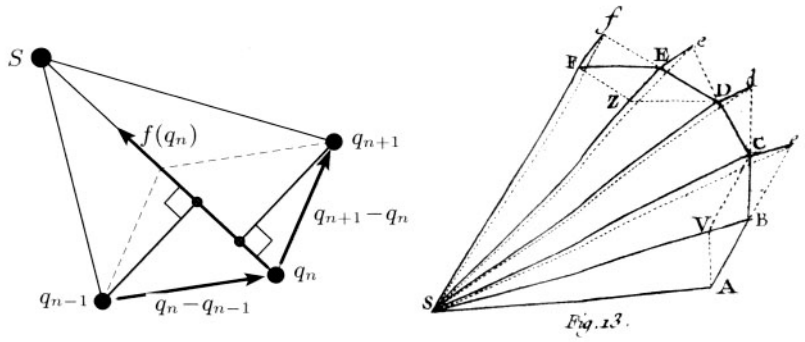

Fig. 2.1. Proof of Kepler's Second Law (left); facsimile from Newton's *Principia* (right)

We have not only an elegant proof for this invariant, but we also see that *the Störmer–Verlet scheme preserves this invariant for every* $h > 0$.

I.2.2 Exact Integration of the Kepler Problem

> Pour voir présentement que cette courbe ABC ... est toûjours une Section Conique, ainsi que Mr. Newton l'a supposé, *pag. 55. Coroll.I.* sans le démontrer; il y faut bien plus d'adresse: (Joh. Bernoulli 1710, p. 475)

It is now interesting, inversely to the procedure of Newton, to prove that *any* solution of (2.2) follows either an elliptic, parabolic or hyperbolic arc and to describe the solutions analytically. This was first done by Joh. Bernoulli (1710, full of sarcasm against Newton), and by Newton (1713, second edition of the *Principia*, without mentioning a word about Bernoulli).

By (2.3) and (2.4), every solution of (2.2) satisfies the two relations

$$\frac{1}{2}\left(\dot{q}_1^2+\dot{q}_2^2\right)-\frac{1}{\sqrt{q_1^2+q_2^2}}=H_0, \qquad q_1\dot{q}_2-q_2\dot{q}_1=L_0, \tag{2.5}$$

where the constants H_0 and L_0 are determined by the initial values. Using polar coordinates $q_1 = r\cos\varphi$, $q_2 = r\sin\varphi$, this system becomes

$$\frac{1}{2}\left(\dot{r}^2+r^2\dot{\varphi}^2\right)-\frac{1}{r}=H_0, \qquad r^2\dot{\varphi}=L_0. \tag{2.6}$$

For its solution we consider r as a function of φ and write $\dot{r} = \frac{dr}{d\varphi}\cdot\dot{\varphi}$. The elimination of $\dot{\varphi}$ in (2.6) then yields

$$\frac{1}{2}\left(\left(\frac{dr}{d\varphi}\right)^2+r^2\right)\frac{L_0^2}{r^4}-\frac{1}{r}=H_0.$$

In this equation we use the substitution $r = 1/u$, $dr = -du/u^2$, which gives (with $' = d/d\varphi$)

$$\frac{1}{2}(u'^2+u^2)-\frac{u}{L_0^2}-\frac{H_0}{L_0^2}=0. \tag{2.7}$$

This is a "Hamiltonian" for the system

$$u'' + u = \frac{1}{d} \quad \text{i.e.,} \quad u = \frac{1}{d} + c_1 \cos\varphi + c_2 \sin\varphi = \frac{1 + e\cos(\varphi - \varphi^*)}{d} \tag{2.8}$$

where $d = L_0^2$ and the constant e becomes, from (2.7),

$$e^2 = 1 + 2H_0 L_0^2 \tag{2.9}$$

(by Exercise 7, the expression $1+2H_0L_0^2$ is non-negative). This is precisely formula (2.1). The angle φ^* is determined by the initial values r_0 and φ_0. Equation (2.1) represents an elliptic orbit with eccentricity e for $H_0 < 0$ (see Fig. 2.2, dotted line), a parabola for $H_0 = 0$, and a hyperbola for $H_0 > 0$.

Finally, we must determine the variables r and φ as functions of t. With the relation (2.8) and $r = 1/u$, the second equation of (2.6) gives

$$\frac{d^2}{\big(1 + e\cos(\varphi - \varphi^*)\big)^2}\, d\varphi = L_0\, dt \tag{2.10}$$

which, after an elementary, but not easy, integration, represents an implicit equation for $\varphi(t)$.

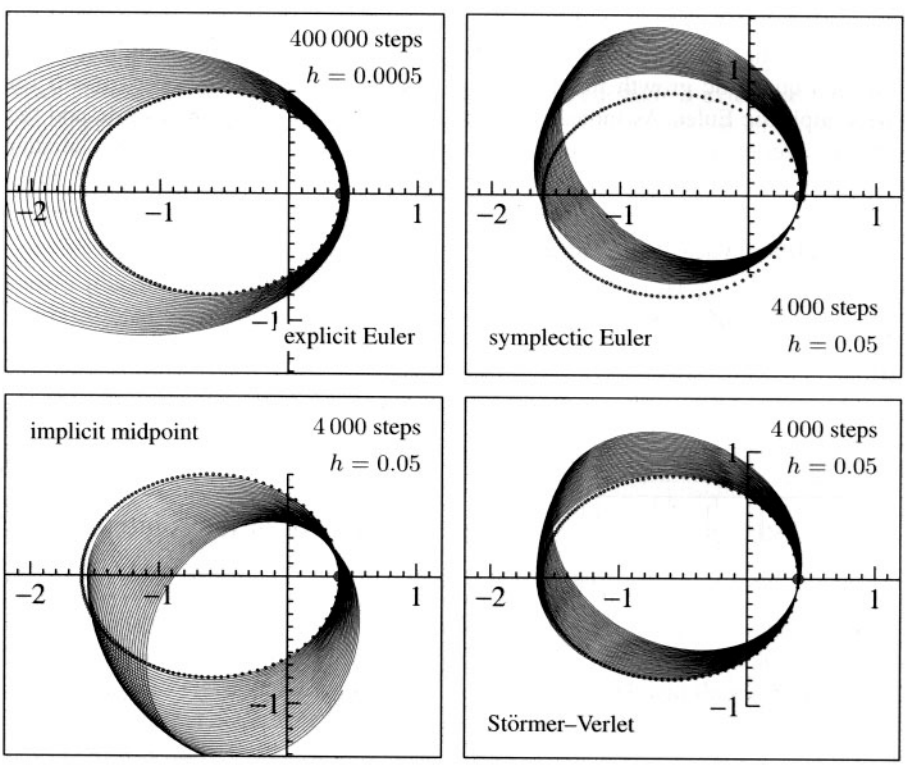

Fig. 2.2. Numerical solutions of the Kepler problem (eccentricity $e = 0.6$; in dots: exact solution)

I.2.3 Numerical Integration of the Kepler Problem

For the problem (2.2) we choose, with $0 \le e < 1$, the initial values

$$q_1(0) = 1 - e, \quad q_2(0) = 0, \quad \dot{q}_1(0) = 0, \quad \dot{q}_2(0) = \sqrt{\frac{1+e}{1-e}}. \tag{2.11}$$

This implies that $H_0 = -1/2$, $L_0 = \sqrt{1-e^2}$, $d = 1 - e^2$ and $\varphi^* = 0$. The period of the solution is 2π (Exercise 5). Fig. 2.2 shows some numerical solutions for the eccentricity $e = 0.6$ compared to the exact solution. After our previous experience, it is no longer a surprise that the explicit Euler method spirals outwards and gives a completely wrong answer. For the other methods we take a step size 100 times larger in order to "see something". We see that the nonsymmetric symplectic Euler method distorts the ellipse, and that all methods exhibit a *precession* effect, clockwise for Störmer–Verlet and symplectic Euler, anti-clockwise for the implicit midpoint rule. The same behaviour occurs for the exact solution of *perturbed* Kepler problems (Exercise 12) and has occupied astronomers for centuries.

Our next experiment (Fig. 2.3) studies the conservation of invariants and the global error. The main observation is that the error in the energy grows linearly for the explicit Euler method, and it remains bounded and small (no secular terms) for the symplectic Euler method. The global error, measured in the Euclidean norm, shows a quadratic growth for the explicit Euler compared to a linear growth for the symplectic Euler. As indicated in Table 2.1 the implicit midpoint rule and the Störmer–Verlet scheme behave similar to the symplectic Euler, but have a smaller

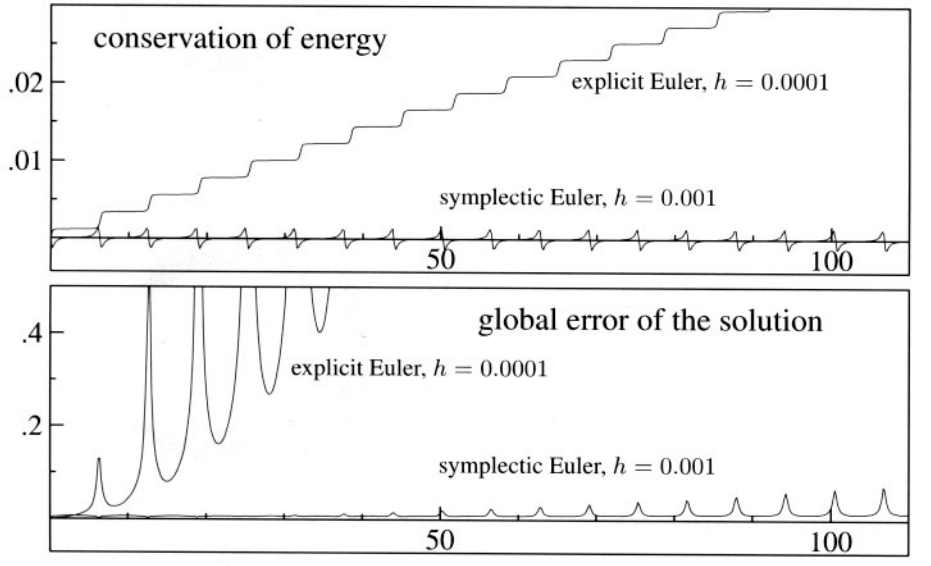

Fig. 2.3. Energy conservation and global error for the Kepler problem

Table 2.1. Qualitative long-time behaviour for the Kepler problem; t is time, h the step size

method	error in H	error in L	global error
explicit Euler	$\mathcal{O}(th)$	$\mathcal{O}(th)$	$\mathcal{O}(t^2h)$
symplectic Euler	$\mathcal{O}(h)$	0	$\mathcal{O}(th)$
implicit midpoint	$\mathcal{O}(h^2)$	0	$\mathcal{O}(th^2)$
Störmer–Verlet	$\mathcal{O}(h^2)$	0	$\mathcal{O}(th^2)$

error due to their higher order. We remark that the angular momentum $L(p,q)$ is exactly conserved by the symplectic Euler, the Störmer–Verlet, and the implicit midpoint rule.

I.2.4 The Outer Solar System

> The evolution of the entire planetary system has been numerically integrated for a time span of nearly 100 million years[5]. This calculation confirms that the evolution of the solar system as a whole is chaotic, ...
>
> (G.J. Sussman & J. Wisdom 1992)

We next apply our methods to the system which describes the motion of the five outer planets relative to the sun. This system has been studied extensively by astronomers. The problem is a Hamiltonian system (1.10) (N-body problem) with

$$H(p,q) = \frac{1}{2}\sum_{i=0}^{5}\frac{1}{m_i}\,p_i^T p_i - G\sum_{i=1}^{5}\sum_{j=0}^{i-1}\frac{m_i\,m_j}{\|q_i - q_j\|}. \tag{2.12}$$

Here p and q are the supervectors composed by the vectors $p_i, q_i \in \mathbb{R}^3$ (momenta and positions), respectively. The chosen units are: masses relative to the sun, so that the sun has mass 1. We have taken

$$m_0 = 1.00000597682$$

to take account of the inner planets. Distances are in astronomical units (1 [A.U.] = 149 597 870 [km]), times in earth days, and the gravitational constant is

$$G = 2.95912208286 \cdot 10^{-4}.$$

The initial values for the sun are taken as $q_0(0) = (0,0,0)^T$ and $\dot{q}_0(0) = (0,0,0)^T$. All other data (masses of the planets and the initial positions and initial velocities) are given in Table 2.2. The initial data is taken from "Ahnerts Kalender für Sternfreunde 1994", Johann Ambrosius Barth Verlag 1993, and they correspond to September 5, 1994 at 0h00.[6]

[5] 100 million years is not much in astronomical time scales; it just goes back to "Jurassic Park".

[6] We thank Alexander Ostermann, who provided us with this data.

Table 2.2. Data for the outer solar system

planet	mass	initial position	initial velocity
Jupiter	$m_1 = 0.000954786104043$	-3.5023653 -3.8169847 -1.5507963	0.00565429 -0.00412490 -0.00190589
Saturn	$m_2 = 0.000285583733151$	9.0755314 -3.0458353 -1.6483708	0.00168318 0.00483525 0.00192462
Uranus	$m_3 = 0.0000437273164546$	8.3101420 -16.2901086 -7.2521278	0.00354178 0.00137102 0.00055029
Neptune	$m_4 = 0.0000517759138449$	11.4707666 -25.7294829 -10.8169456	0.00288930 0.00114527 0.00039677
Pluto	$m_5 = 1/(1.3 \cdot 10^8)$	-15.5387357 -25.2225594 -3.1902382	0.00276725 -0.00170702 -0.00136504

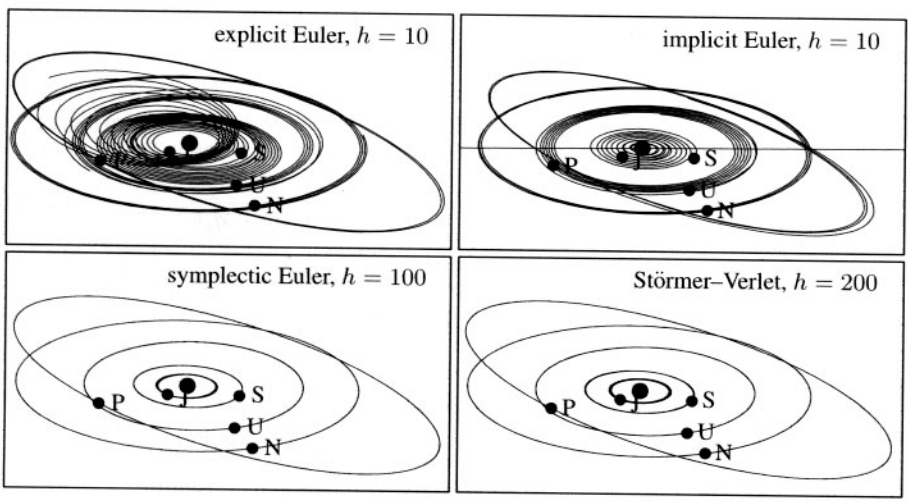

Fig. 2.4. Solutions of the outer solar system

To this system we apply the explicit and implicit Euler methods with step size $h = 10$, the symplectic Euler and the Störmer–Verlet method with much larger step sizes $h = 100$ and $h = 200$, repectively, all over a time period of 200 000 days. The numerical solution (see Fig. 2.4) behaves similarly to that for the Kepler problem. With the explicit Euler method the planets have increasing energy, they spiral outwards, Jupiter approaches Saturn which leaves the plane of the two-body motion. With the implicit Euler method the planets (first Jupiter and then Saturn)

fall into the sun and are thrown far away. Both the symplectic Euler method and the Störmer–Verlet scheme show the correct behaviour. An integration over a much longer time of say several million years does not deteriorate this behaviour. Let us remark that Sussman & Wisdom (1992) have integrated the outer solar system with special geometric integrators.

I.3 The Hénon–Heiles Model

> . . . because: (1) it is analytically simple; this makes the computation of the trajectories easy; (2) at the same time, it is sufficiently complicated to give trajectories which are far from trivial . (Hénon & Heiles 1964)

The Hénon–Heiles model was created for describing stellar motion, followed for a very long time, inside the gravitational potential $U_0(r, z)$ of a galaxy with cylindrical symmetry (Hénon & Heiles 1964). Extensive numerical experimentations should help to answer the question, if there exists, besides the known invariants H and L, a *third* invariant. Despite endless tentatives of analytical calculations during many decades, such a formula had not been found.

After a reduction of the dimension, a Hamiltonian in two degrees of freedom of the form

$$H(p, q) = \frac{1}{2}(p_1^2 + p_2^2) + U(q) \tag{3.1}$$

is obtained and the question is, if such an equation has a *second* invariant. Here, Hénon and Heiles put aside the astronomical origin of the problem and choose

$$U(q) = \frac{1}{2}(q_1^2 + q_2^2) + q_1^2 q_2 - \frac{1}{3}q_2^3 \tag{3.2}$$

(see citation). The potential U is represented in Fig. 3.1. When U approaches $\frac{1}{6}$, the level curves of U tend to an equilateral triangle, whose vertices are saddle points of U. The corresponding system

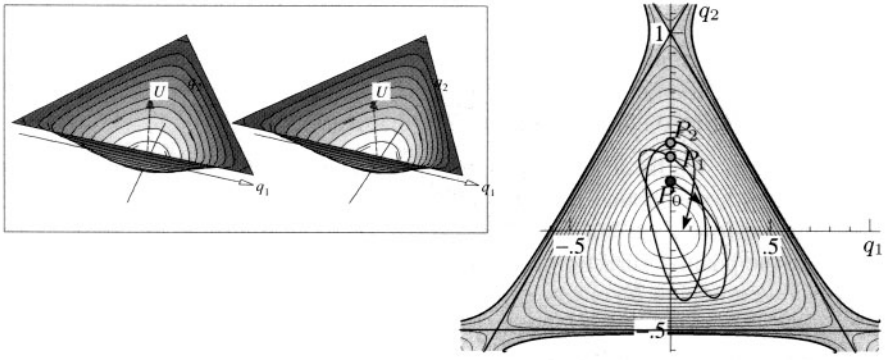

Fig. 3.1. Potential of the Hénon–Heiles Model and a solution

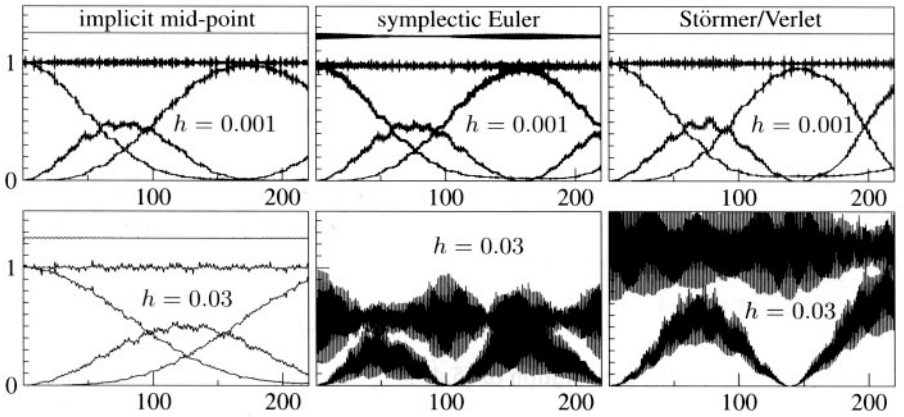

Fig. 5.3. Numerical solution for the FPU problem (5.2) with data as in Sect. I.5.1, obtained with the implicit midpoint rule (left), symplectic Euler (middle), and Störmer–Verlet scheme (right); the upper pictures use $h = 0.001$, the lower pictures $h = 0.03$; the first four pictures show the Hamiltonian $H - 0.8$ and the oscillatory energies I_1, I_2, I_3, I; the last two pictures only show I_2 and I

to the stability limit of the symplectic Euler and the Störmer–Verlet methods. The values of H and I are still bounded over very long time intervals, but the oscillations do not represent the true behaviour. Moreover, the average value of I is no longer close to 1, as it is for the exact solution. These phenomena call for an explanation, and for numerical methods with an improved behaviour (see Chap. XIII).

I.6 Exercises

1. Show that the Lotka–Volterra problem (1.1) in logarithmic scale, i.e., by putting $p = \log u$ and $q = \log v$, becomes a Hamiltonian system with the function (1.4) as Hamiltonian (see Fig. 6.1).

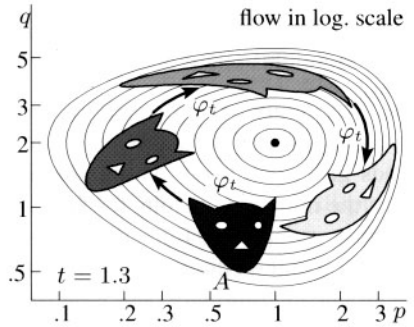

Fig. 6.1. Area preservation in logarithmic scale of the Lotka–Volterra flow

2. Apply the symplectic Euler method (or the implicit midpoint rule) to problems such as

$$\begin{pmatrix} \dot{u} \\ \dot{v} \end{pmatrix} = \begin{pmatrix} (v-2)/v \\ (1-u)/u \end{pmatrix}, \qquad \begin{pmatrix} \dot{u} \\ \dot{v} \end{pmatrix} = \begin{pmatrix} u^2 v(v-2) \\ v^2 u(1-u) \end{pmatrix}$$

with various initial conditions. Both problems have the same first integral (1.4) as the Lotka–Volterra problem and therefore their solutions are also periodic. Do the numerical solutions also show this behaviour?

3. A general two-body problem (sun and planet) is given by the Hamiltonian

$$H(p, p_S, q, q_S) = \frac{1}{2M} p_S^T p_S + \frac{1}{2m} p^T p - \frac{GmM}{\|q - q_S\|},$$

where $q_S, q \in \mathbb{R}^3$ are the positions of the sun (mass M) and the planet (mass m), $p_S, p \in \mathbb{R}^3$ are their momenta, and G is the gravitational constant.
a) Prove: in heliocentric coordinates $Q := q - q_S$, the equations of motion are

$$\ddot{Q} = -G(M+m)\frac{Q}{\|Q\|^3}.$$

b) Prove that $\frac{d}{dt}\big(Q(t) \times \dot{Q}(t)\big) = 0$, so that $Q(t)$ stays for all times t in the plane $E = \{q\,;\, d^T q = 0\}$, where $d = Q(0) \times \dot{Q}(0)$.
Conclusion. The coordinates corresponding to a basis in E satisfy the two-dimensional equations (2.2).

4. In polar coordinates, the two-body problem (2.2) becomes

$$\ddot{r} = -V'(r) \qquad \text{with} \qquad V(r) = \frac{L_0^2}{2r^2} - \frac{1}{r}$$

which is independent of φ. The angle $\varphi(t)$ can be obtained by simple integration from $\dot{\varphi}(t) = L_0/r^2(t)$.

5. Compute the period of the solution of the Kepler problem (2.2) and deduce from the result Kepler's "third law".
Hint. Comparing Kepler's second law (2.6) with the area of the ellipse gives $\frac{1}{2} L_0 T = ab\pi$. Then apply (2.7). The result is $T = 2\pi(2|H_0|)^{-3/2} = 2\pi a^{3/2}$.

6. Deduce Kepler's first law from (2.2) by the elegant method of Laplace (1799).
Hint. Multiplying (2.2) with (2.5) gives

$$L_0 \ddot{q}_1 = \frac{d}{dt}\Big(\frac{q_2}{r}\Big), \qquad L_0 \ddot{q}_2 = \frac{d}{dt}\Big(-\frac{q_1}{r}\Big),$$

and after integration $L_0 \dot{q}_1 = \frac{q_2}{r} + B$, $L_0 \dot{q}_2 = -\frac{q_1}{r} + A$, where A and B are integration constants. Then eliminate $\dot{q}_1$ and $\dot{q}_2$ by multiplying these equations by q_2 and $-q_1$ respectively and by subtracting them. The result is a quadratic equation in q_1 and q_2.

7. Whatever the initial values for the Kepler problem are, $1 + 2H_0 L_0^2 \geq 0$ holds. Hence, the value e is well defined by (2.9).
Hint. L_0 is the area of the parallelogram spanned by the vectors $q(0)$ and $\dot{q}(0)$.

8. *Implementation of the Störmer–Verlet scheme.* Explain why the use of the one-step formulation (1.17) is numerically more stable than that of the two-term recursion (1.15).
9. *Runge–Lenz–Pauli vector.* Prove that the function

$$A(p,q) = \begin{pmatrix} p_1 \\ p_2 \\ 0 \end{pmatrix} \times \begin{pmatrix} 0 \\ 0 \\ q_1 p_2 - q_2 p_1 \end{pmatrix} - \frac{1}{\sqrt{q_1^2+q_2^2}} \begin{pmatrix} q_1 \\ q_2 \\ 0 \end{pmatrix}$$

is a first integral of the Kepler problem, i.e., $A\big(p(t),q(t)\big) = Const$ along solutions of the problem. However, it is not a first integral of the perturbed Kepler problem of Exercise 12.
10. Add a column to Table 2.1 which shows the long-time behaviour of the error in the Runge–Lenz–Pauli vector (see Exercise 9) for the various numerical integrators.
11. For the Kepler problem, eliminate (p_1, p_2) from the relations $H(p,q) = Const$, $L(p,q) = Const$ and $A(p,q) = Const$. This gives a quadratic relation for (q_1, q_2) and proves that the solution lies on an ellipse, a parabola, or on a hyperbola.
12. Study numerically the solution of the perturbed Kepler problem with Hamiltonian

$$H(p_1,p_2,q_1,q_2) = \frac{1}{2}\left(p_1^2+p_2^2\right) - \frac{1}{\sqrt{q_1^2+q_2^2}} - \frac{\mu}{3\sqrt{(q_1^2+q_2^2)^3}},$$

where μ is a positive or negative small number. Among others, this problem describes the motion of a planet in the Schwarzschild potential for Einstein's general relativity theory[7]. You will observe a precession of the perihelion, which, applied to the orbit of Mercury, represented the historically first verification of Einstein's theory (see e.g., Birkhoff 1923, p. 261-264).

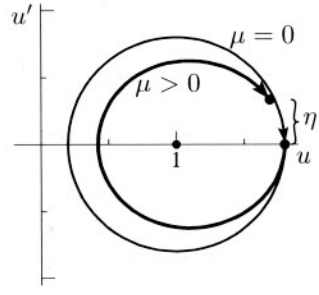

The precession can also be expressed analytically: the equation for $u = 1/r$ as a function of φ, corresponding to (2.8), here becomes

$$u'' + u = \frac{1}{d} + \mu u^2, \tag{6.1}$$

where $d = L_0^2$. Now compute the derivative of this solution with respect to μ, at $\mu = 0$ and $u = (1 + e\cos(\varphi - \varphi^*))/d$ after one period $t = 2\pi$. This leads to $\eta = \mu(e/d^2)\cdot 2\pi \sin\varphi$ (see the small picture). Then, for small μ, the precession after one period is

$$\Delta\varphi = \frac{2\pi\mu}{d}. \tag{6.2}$$

[7] We are grateful to Prof. Ruth Durrer for helpful hints about this subject.